Anal. Chem. **2008,** *80,* 8545–8553

Resonance Energy Transfer-Amplifying Fluorescence Quenching at the Surface of Silica Nanoparticles toward Ultrasensitive Detection of TNT

Daming Gao,[†,‡] Zhenyang Wang,[†] Bianhua Liu,[†] Lin Ni,[†] Minghong Wu,[§] and Zhongping Zhang*[,†]

Key Laboratory of Biomimetic Sensing & Advanced Robot Technology, Institute of Intelligent Machines, Chinese Academy of Sciences, Hefei, Anhui 230031, China, Department of Chemistry, University of Science & Technology of China, Hefei, Anhui 230026, China, and Institute of Nanochemistry & Biology, Shanghai University, 99 Shangda Road, Shanghai 200436, China

This paper reports a resonance energy transfer-amplifying fluorescence quenching at the surface of silica nanoparticles for the ultrasensitive detection of 2,4,6-trinitrotoluene (TNT) in solution and vapor environments. Fluorescence dye and organic amine were covalently modified onto the surface of silica nanoparticles to form a hybrid monolayer of dye fluorophores and amine ligands. The fluorescent silica particles can specifically bind TNT species by the charge-transfer complexing interaction between electron-rich amine ligands and electron-deficient aromatic rings. The resultant TNT−amine complexes bound at the silica surface can strongly suppress the fluorescence emission of the chosen dye by the fluorescence resonance energy transfer (FRET) from dye donor to the irradiative TNT−amine acceptor through intermolecular polar−polar interactions at spatial proximity. The quenching efficiency of the hybrid nanoparticles with TNT is greatly amplified by at least 10-fold that of the corresponding pure dye. The nanoparticle-assembled arrays on silicon wafer can sensitively detect down to ~1 nM TNT with the use of only 10 μL of solution (~2 pg TNT) and several ppb of TNT vapor in air. The simple FRET-based nanoparticle sensors reported here exhibit a high and stable fluorescence brightness, strong analyte affinity, and good assembly flexibility and can thus find many applications in the detection of ultratrace analytes.

The powerful explosivity and deleterious pollution of nitroaromatic compounds have concurrently raised worldwide concerns of public security and environmental problem, due to their wide production and use as explosives in the military and in engineering. The presently used detections of nitroaromatics are usually time-consuming with the employment of cumbersome and expensive gas chromatography coupled to a mass spectrometer, ion mobility spectrometry, and neutron activation analysis.[1] Therefore, the development of ultrasensitive chemosensors for the real-time detection of nitroaromatics has attracted considerable research efforts in recent years.[2−11] In principle, the detection sensitivity is mainly dependent on the transduction approaches to signal the analyte binding at sensory materials and on the interaction manners between sensory materials and target analytes. Of various signal transducers, fluorescence quenching-based chemosensors, where analyte binding produces an attenuation in the light emission, are best suited for the detection of nitroaromatics because the electron-deficient nitro compounds are the strong quenchers of electron-rich fluorophores via a charge-transfer mechanism. Recently, conjugated polymers have most extensively been explored as chemosensory materials for the fluorescence detection of electron-deficient analytes such as 2,4,6-trinitrotoluene (TNT).[4−6] Swager et al. reported the amplified fluorescence quenching to the nitroaromatic binding events in the aggregated systems and solid films of conjugated polymers through intermolecular exciton migration,[4,5] and the multiphoton fluorescence quenching,[6] providing an ultrasensitive detection of TNT. More recently, molecular imprinting in the matrix of conjugated polymers could further improve the chemoselectivity to nitroaro-

* To whom correspondence should be addressed. E-mail: zpzhang@iim.ac.cn.
[†] Chinese Academy of Sciences.
[‡] University of Science & Technology of China.
[§] Shanghai University.

(1) Steinfeld, J. I.; Wormhoudt, J. *Annu. Rev. Phys. Chem.* **1998**, *49*, 203.
(2) Toal, S. J.; Trogler, W. C. *J. Mater. Chem.* **2006**, *16*, 2871.
(3) Pushkarsky, M. B.; Dunayevskiy, I. G.; Prasanna, M.; Tsekoun, A. G.; Go, R.; Patel, C. K. N. *Proc. Natl. Acad. Sci.U. S. A.* **2006**, *103*, 19630.
(4) Rose, A.; Zhu, Z.; Madigan, C. F.; Swager, T. M.; Bulovic, V. *Nature* **2005**, *434*, 876.
(5) (a) Yang, J-S.; Swager, T. M. *J. Am. Chem. Soc.* **1998**, *120*, 11864. (b) Zahn, S.; Swager, T. M. *Angew. Chem., Int. Ed.* **2002**, *41*, 4226. (c) Yamaguchi, S.; Swager, T. M. *J. Am. Chem. Soc.* **2001**, *123*, 12087. (d) Yang, J-S.; Swager, T. M. *J. Am. Chem. Soc.* **1998**, *120*, 5321.
(6) Narayanan, A.; Varnavski, O. P.; Swager, T. M.; Goodson III, T. *J. Phys. Chem. C* **2008**, *112*, 881.
(7) Li, J. H.; Kendig, C. E.; Nesterov, E. E. *J. Am. Chem. Soc.* **2007**, *129*, 15911.
(8) (a) Goldman, E. R.; Medintz, I. L.; Whitley, J. L.; Hayhurst, A.; Clapp, A. R.; Uyeda, H. T.; Deschamps, J. R.; Lassman, M. E.; Mattoussi, H. *J. Am. Chem. Soc.* **2005**, *127*, 6744. (b) Medintz, I. L.; Goldman, E. R.; Lassman, M. E.; Hayhurst, A.; Kusterbeck, A. W.; Deschamps, J. R. *Anal. Chem.* **2005**, *77*, 365.
(9) Tu, R. Y.; Liu, B. H.; Wang, Z. Y.; Gao, D. M.; Wang, F.; Fang, Q. L.; Zhang, Z. P. *Anal. Chem.* **2008**, *80*, 3458.
(10) Xie, C. G.; Liu, B. H.; Wang, Z. Y.; Gao, D. M.; Guan, G. J.; Zhang, Z. P. *Anal. Chem.* **2008**, *80*, 437.
(11) (a) Gao, D. M.; Zhang, Z. P.; Wu, M. H.; Xie, C. G.; Guan, G. J.; Wang, D. P. *J. Am. Chem. Soc.* **2007**, *129*, 7859. (b) Guan, G. J.; Zhang, Z. P.; Wang, Z. Y.; Liu, B. H.; Gao, D. M.; Xie, C. G. *Adv. Mater.* **2007**, *19*, 2370. (c) Xie, C. G.; Zhang, Z. P.; Wang, D. P.; Guan, G. J.; Gao, D. M.; Liu, J. H. *Anal. Chem.* **2006**, *78*, 8339.

10.1021/ac8014356 CCC: $40.75
Published on Web 10/11/2008

matic analytes.[7] Other photoluminescent materials such as poly(tetraphenylsilole),[12] poly(tetraphenylgermole),[13] photoluminescent silica films,[14] and silica microspheres with physisorbed dyes[15] have also been used for the fluorescence detection of nitroaromatic explosives through the charge-transfer quenching mechanism.

However, it would be naturally conceivable to develop the fluorescence-based sensors with high chemoselectivity to target analytes. The "lab-on-nanoparticles" concept has recently provided the practical possibility for the development of novel fluorescence chemosensors. [16,17] The high selectivity and sensitivity may be simultaneously achieved by the predesigned assembly of specific receptors (binding the target species) and efficient transducers (signaling the binding events) at the surface of nanoparticles/quantum dots (QDs).[8,9] A typical example is that the QD chemosensors based on fluorescence resonance energy transfer (FRET) have been made by the chemical immobilization of dye molecules and biological receptors at the surface of photoluminescent QDs.[8,18−20] The specific binding of target analyte with antibody interrupts the FRET between QDs and dyes at spatial proximity, providing a sensitive response to the target analyte. For example, the CdSe quantum dots modified by TNT antibody segments and dye molecules can selectively detect trace TNT species in solution.[8] Recently, the principle of FRET-based nanoparticle sensors has been successfully extended to the detection of maltose,[18] DNA,[19] and enzyme activities.[20]

Until now, most of FRET-based chemosensors are usually involved in the use of two photoluminescent elements with an approximate energy band gap, in which the fluorescent emission of a donor is transferred to an acceptor and thus excites the fluorescence of the acceptor. However, the FRET from a photoluminescent donor to a nonemissive analyte receptor for direct chemodetection of the analyte has thus far rarely been explored. In principle, if the absorption band of an analyte (or its derivatives) overlaps with the emission band of a fluorescent dye, the resonance energy transfer by the polar−polar interactions at a spatial proximity will result in the superquenching of donor fluorescence,[21] which may provide a facile and ultrasensitive detection of target analytes. Herein, we reported the resonance energy transfer-amplifying fluorescence quenching of dye at the surface of silica nanoparticles for the ultrasensitive detection of TNT. Silica nanoparticles are particularly suited for the realization of the FRET-based chemosensors, because they are optically transparent and photophysically inert, and their surface can easily be modified by the coupling reactions with alkoxysilane derivatives. Fluorescent dye molecules together with primary amine TNT-binding sites were covalently anchored onto the surface of silica nanoparticles, allowing the formation of a hybrid organic monolayer (dye-(NH_2)-silica). The specific binding of TNT with the amine ligands leads to the formation of TNT−amine complexes at the surface of silica particles, which strongly suppresses the fluorescence emission of the proximally positioned marker dye through the resonance energy transfer from the chosen dye to the TNT derivatives. The amplifying fluorescence quenching can sensitively detect the ultratrace TNT in solution and atmosphere, and selectively distinguish different types of nitro compounds.

EXPERIMENTAL SECTION

Materials. Tetraethylorthosilicate (TEOS), 3-aminopropyltriethoxysilane (APTS), fluorescein 5(6)-isothiocyanate (FITC), and 6-carboxy-X-rhodamine *N*-succinimidyl ester (ROX) were used as received from Sigma-Aldrich. TNT and 1,3,5-trinitro-1,3,5-triazinane (RDX) were supplied by National Security Department of China and recrystallized with ethanol before use. 2,4-Dinitrotoluene (DNT) was purchased from Merch-Schuchardt (Hohenbrunn, Germany). Ammonium hydroxide (25%), absolute ethanol, acetronitrile, and nitrobenzene (NB) were purchased from Shanghai Chemicals Ltd.

Caution: The highly explosive TNT and RDX should be used with extreme caution and handled only in small quantities.

Synthesis of Dye-(NH_2)-Silica and Dye-Silica Nanoparticles. Uniform silica nanoparticles with a size of 200 nm were synthesized by the hydrolysis of TEOS with aqueous ammonia, according to the reported Stöber method.[22] To prepare the silica nanoparticles with a hybrid monolayer of dye and amine ligand (dye-(NH_2)-silica), the FITC or ROX dye with coupling groups were first conjugated with APTS by an addition reaction of amine group with isothiocyanate or a succinimidyl group. The reaction was carried out in dark for at least 12 h by slowly stirring the solution containing the dye and an excess of APTS in anhydrous ethanol. Humidity was excluded by inputting dry nitrogen to prevent the hydrolysis and condensation of APTS itself. Typically, 2.4 mg of FITC dye was dissolved in anhydrous alcohol containing an excess of APTS (0.5 mL) and stirred under a dry nitrogen atmosphere, leading to the formation of FITC−APTS conjugates in the mixture solution. Subsequently, 10 mL of the above solution containing APTS and FITC−APTS conjugates was added into 100 mL of suspension of monodisperse silica particles. The anchoring reaction of APTS and FITC−APTS conjugates at the surface of silica particles was carried out by stirring the mixture solution at room temperature for 24 h.[11a] After the product was separated by centrifugation and washing with ethanol, FITC-(NH_2)-silica nanoparticles with a hybrid monolayer of FITC dye and free amine ligands at the surface were finally obtained and then redispersed in ethanol for further use. ROX-(NH_2)-silica nanoparticles were

(12) (a) Toal, S. J.; Magde, D.; Trogler, W. C. *Chem. Commun.* **2005**, 5465. (b) Sohn, H.; Calhoun, R. M.; Sailor, M. J.; Trogler, W. C. *Angew. Chem., Int. Ed.* **2001**, *40*, 2104.

(13) Sohn, H.; Sailor, M. J.; Magde, D.; Trogler, W. C. *J. Am. Chem. Soc.* **2003**, *125*, 3821.

(14) Content, S.; Trogler, W. C.; Sailor, M. J. *Chem. Eur. J.* **2000**, *6*, 2205.

(15) Albert, K. J.; Walt, D. R. *Anal. Chem.* **2000**, *72*, 1947.

(16) (a) Medintz, I. L.; Uyeda, H. T.; Goldman, E. R.; Mattoussi, H. *Nat. Mater.* **2005**, *4*, 435. (b) Han, M. Y.; Gao, X. H.; Su, J. Z.; Nie, S. M. *Nat. Biotechnol.* **2001**, *19*, 631.

(17) (a) Burns, A.; Ow, H.; Wiesner, U. *Chem. Soc. Rev.* **2006**, *35*, 1028. (b) Rampazzo, E.; Brasola, E.; Marcuz, S.; Mancin, F.; Tecilla, P.; Tonellato, U. *J. Mater. Chem.* **2005**, *15*, 2687. (c) Corrie, S. R.; Lawrie, G. A.; Trau, M. *Langmuir* **2006**, *22*, 2731. (d) Ow, H.; Larson, D. R.; Srivastava, M.; Baird, B. A.; Webb, W. W.; Wiesner, U. *Nano Lett.* **2005**, *5*, 113. (e) Burns, A.; Sengupta, P.; Zedayko, T.; Baird, B.; Wiesner, U. *Small* **2006**, *2*, 732.

(18) Medintz, I. L.; Clapp, A. R.; Brunel, F. M.; Tiefenbrunn, T.; Uyeda, H. T.; Chang, E. L.; Deschamps, J. R.; Dawson, P. E.; Mattoussi, H. *Nat. Mater.* **2006**, *5*, 581.

(19) Peng, H.; Zhang, L. J.; Kjällman, T. H. M.; Soeller, C.; Travas-sejdic, J. *J. Am. Chem. Soc.* **2007**, *129*, 3048.

(20) Shi, L. F.; Paoli, V. D.; Rosenzweig, N.; Rosenzweig, Z. *J. Am. Chem. Soc.* **2006**, *128*, 10378.

(21) (a) Lakowicz, J. R. *Principles of Fluorescence Spectroscopy*; Plenum: New York, 1983. (b) Allen, J. F.; Sanders, C. E.; Holmes, N. G. *FEBS Lett.* **1985**, *193*, 271. (c) Kobayshi, Y.; Sasaki, H. *Thin Solid Films* **1991**, *200*, 321.

(22) Stöber, W.; Finker, A.; Bohn, E. *J. Colloid Interface Sci.* **1968**, *26*, 62.

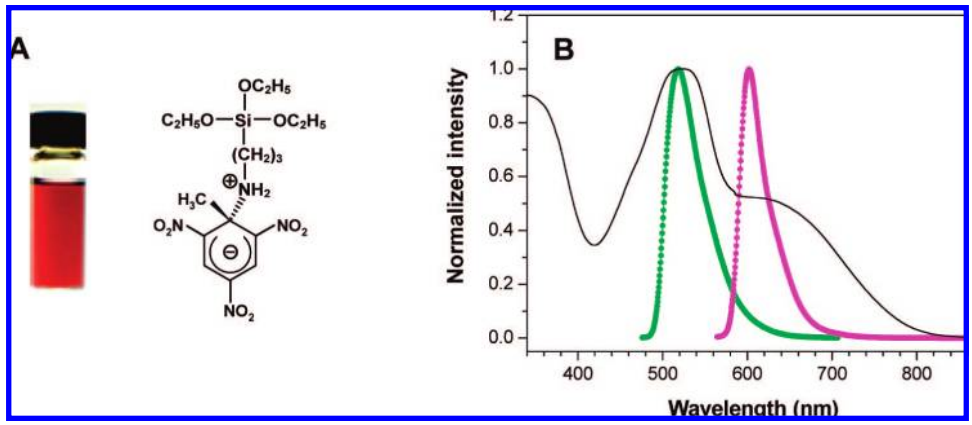

Figure 1. (A) Interaction between TNT and APTS amine through the charge-transfer mechanism to form the red TNT−amine complex in solution (inset image, solvent: ethanol/acetronitrile, 8:2). (B) Normalized absorption spectrum of TNT−APTS solution (black line) plotted together with normalized emission spectra of FITC (green dot line) and ROX (red dot line) dyes.

synthesized according to an identical procedure. As a control sample, the FITC−silica and ROX−silica nanoparticles without free amine ligands were also prepared according to the aforementioned reaction steps, but dye was in excess over APTS, which resulted in a pure monolayer of dye molecules at the surface of silica particles. The excess of FITC or ROX dye was finally removed by washing the products with ethanol.

Measurements of Fluorescence Response to Nitroaromatics. The concentration of stock solution of dye-(NH_2)-silica nanoparticles for the measurements of fluorescence quenching was 2 mg/mL in ethanol. Typically, 20 μL of the stock solution was added to a spectrophotometer quartz cuvette. Subsequently, 2 mL of the known concentration of analyte (solvent: ethanol/acetronitrile, 8:2, v/v) was injected into the above cuvette. The final amount of nanoparticles was ~40 μg of particles in 2 mL of solvent. Fluorescence spectra were recorded immediately after fully mixing the analyte with dye-(NH_2)-silica nanoparticles in solution. Meanwhile, the fluorescence responses of dye−silica nanoparticles and pure dyes to nitroaromatics were also measured by the identical procedure.

Fluorescence lifetime spectra of FITC-(NH_2)-silica nanoparticles were measured by a time-correlated single-photon counting. A neodymium/vanadate laser at 530 nm (Coherent Verdi) pumped a titanium/sapphire laser that generated femtosecond mode-locked pulses by self-phase-locking. The fluorescence emission was collected and sent through a 0.5-m monochromator (Spex 1870) to a micro channel plate photomultiplier (Hamamatsu1564U-01). The fluorescence decay constants were obtained using a mixture solution containing 50 μL of fluorescent silica nanoparticles and 2 mL of TNT solutions of various concentrations.

Before the measurements of fluorescent sensitivity to nitroaromatic vapors, the suspension of FITC-(NH_2)-silica nanoparticles were first coated onto a piece of filter film (1×2 cm^2) and dried at ambient temperature. Small granules or liquid drops of nitro analytes were placed on the bottom of a sealed testing box with two quartz windows and a small slot. Meanwhile, a small cotton gauze was tucked into the testing box to help maintain a constant vapor pressure of analyte.[5] The saturated vapor of nitro compound was produced in the sealed box after 24 h at room temperature. The filter film with FITC-(NH_2)-silica nanoparticles was fixed onto a sample holder that tightly matched with the slot of the testing box and promptly inserted through the slot into the testing box filled up with the saturated vapor. The evolution of fluorescence spectra was recorded every 30 s after exposing the film to the vapor of analyte.

Nanoparticle-Assembled Chips for Ultratrace Detection of TNT. The monodisperse FITC-(NH_2)-silica nanoparticles were assembled into an etched microwell array on a silicon wafer. Briefly, a standard photolithographic technique was used to fabricate the microwell array. PMMA photoresist was first spin-coated onto the surface of a silicon wafer. After exposed to UV light under a photomask, the silicon wafer was immersed into the developing solution to form a pattern of dot array. The microwells of 5 μm in diameter and 2 μm in depth were then etched using Plasmalab System 100 (Oxford Instruments). After the remaining photoresist was removed using acetone, the aqueous suspension of FITC-(NH_2)-silica nanoparticles was cast onto the etched silicon chip and dried under ambient condition. The microwells were spontaneously filled with the silica nanoparticles. The excessive residue at the surface of silicon chip was removed by gently polishing with filter paper. The fluorescence sensitivity to the ultratrace amount of TNT was tested by dropping a microamount of TNT solution onto the silicon chips, and then the fluorescence images of dot arrays were taken using a laser confocal microscope.

Characterizations. The morphology of silica nanoparticles was examined by FEI Sirion-200 field emission scanning electron microscope (SEM) and JEOL 2010 transmission electron microscope (TEM). UV−visible absorbance spectra were obtained by UNIC UV-4802 diode array spectrometer. Fluorescence emission and excitation spectra were recorded using Perkin-Elmer luminescence spectrometer LS-45. Confocal fluorescence images were taken under 488-nm argon ion laser excitation with an Olympus FV1000 confocal microscope.

RESULTS AND DISCUSSION

FRET Mechanism between Dyes and TNT Derivatives. TNT is almost colorless in solution and does not absorb any visible light. Our previous works[9−11] have shown that the solution of TNT changes from colorless to deep red with addition of organic amines such as APTS (colorful image in Figure 1A). A strong charge-transfer interaction, as a predominant process, occurs between the electron-deficient aromatic ring of TNT and the electron-rich amino group of APTS. The electron transfer from amino groups

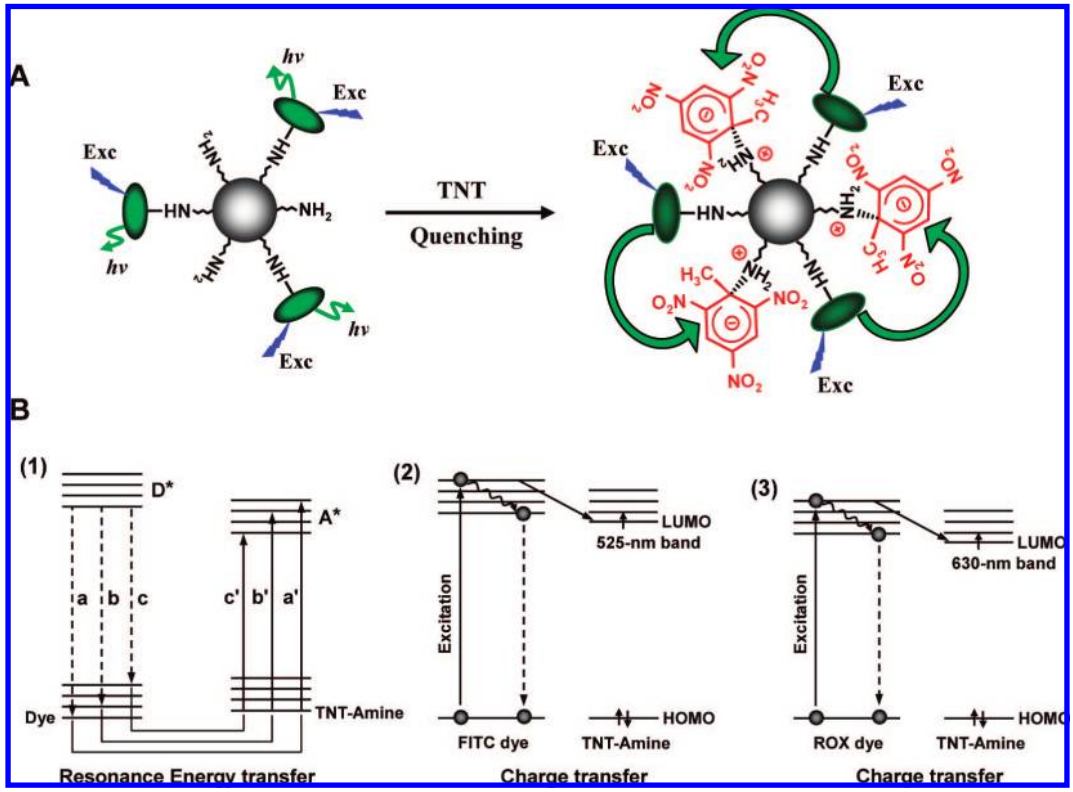

Figure 2. (A) Schematic illustration of the FRET-based silica nanoparticle sensors for TNT detection. (B) Quenching mechanism through (1) resonance energy transfer from FITC/ROX donor to TNT−amine complex acceptor and (2, 3) charge transfers from the excited FITC and ROX dyes to TNT−amine complex, respectively.

to aromatic rings leads to the formation of a Meisenheimer complex between TNT and the primary amine group,[11,23] as illustrated in Figure 1A. The zwitterion complex is a resonance-stabilizing form due to three electron-withdrawing nitro groups and can strongly absorb the green part of visible light. Therefore, the color of solution changes into deep red.

The absorbance spectrum of TNT−APTS solution shows a strong visible absorption with λ_{max} at 525 nm and a weak absorption shoulder with λ_{max} at 630 nm, as plotted with the black line in Figure 1B. We thus chose the FITC dye with a green fluorescence emission at ~518 nm as an energy donor, which has a spectral overlapping with the absorption peak of TNT−amine complexes at 525 nm. Meanwhile, the ROX dye with a red fluorescence emission at ~602 nm was used as a contrast with FITC dye, which has a spectral overlap with the absorption peak of TNT−amine complexes at 630 nm. Figure 1B shows the normalized emission spectra of FITC and ROX dyes, plotted together with the normalized absorption spectrum of TNT−APTS solution. The green dotted line in Figure 1B shows that the main absorption band of TNT−amine complexes has a whole spectral overlapping with the emission band of FITC dyes. This suggests that the resonance energy transfer from FITC molecules to the TNT derivatives may occur if the dye fluorophores and TNT derivatives are spatially close to each other. The fluorescence emission of FITC molecules is strongly absorbed by the TNT derivatives, resulting in the nonemissive resonance transfer-based fluorescence quenching. On the other hand, the emission band of the ROX dye (red dotted line in Figure 1B) only exhibits a partial spectral overlapping with the weak absorption shoulder of the TNT derivatives, due to the small extinction coefficient of TNT derivatives at this emission wavelength of ROX. It is thus expected that the FITC dye should show a much stronger quenching response with TNT than ROX dye, according to the FRET mechanism. The efficiency of the energy transfer is mainly dependent on the degree of spectral overlapping between the emission of dye donor and the absorption of analyte acceptor.

FRET-Based Silica Nanoparticle Sensors for TNT Detection. Figure 2A shows the schematic drawing of a dye-(NH_2)-silica nanoparticle sensor for TNT detection. The FITC/ROX dye and APTS amine were covalently linked onto the surface of silica nanoparticles by the reaction of alkoxysilane derivatives with silica surfaces.[11a] The primary amine ligands at the surface of silica particles play the role of recognition receptor of TNT molecules by the strong specific interactions mentioned above.[9] TNT analyte is thus attached onto the surface of silica particles in the form of a TNT−amine complex. The analyte binding will lead to the quenching of dye fluorescence through two possible pathways: the resonance energy transfer and the common charge transfer from dye to TNT−amine complex. Part 1 of Figure 2B illustrates the quenching mechanism of FITC/ROX fluorescence through the resonance energy transfer from dye donor to TNT−amine acceptor. The exciting band gap of the chosen dyes is about equal to the absorption band gap of the TNT−amine complex, and they are of spatial proximity at the surface of nanoparticle. When the excited-state electrons of the dye donor return to ground state through the pathway of a, b, and c, the ground-state electrons of the TNT−amine complex thus transit to the excited states through

(23) (a) Lowry, T. H.; Richardson, K. S. *Mechanism and Theory in Organic Chemistry*; Benjamin-Cummins: New York, 1987. (b) Meisenheimer, J. *Justus Liebigs Ann. Chem.* **1902**, *323*, 205.

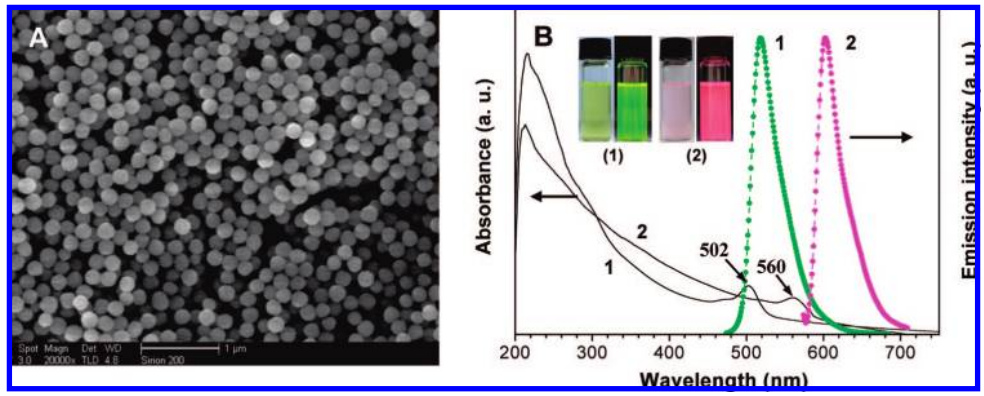

Figure 3. (A) SEM image of dye-(NH_2)-silica nanoparticles. (B) The absorption and emission spectra of (1) FITC-(NH_2)-silica and (2) ROX-(NH_2)-silica nanoparticle solution. The inset shows the optical images of (1) FITC-(NH_2)-silica and (2) ROX-(NH_2)-silica particle solutions under natural light (left) and under 360-nm UV lamp (right), respectively.

the corresponding pathway of a′, b′, and c′, respectively, due to the polar−polar resonance of donor and acceptor. The coupling transitions will result in the highly efficient quenching of dye fluorescence. On the other hand, it should be noted that the fluorescences of FITC and ROX molecules may also be quenched by the charge-transfer mechanism, as illustrated in parts 2 and 3 of Figure 2B, respectively. Because the 525-nm absorption band of TNT−amine complex overlaps with the emission band of FITC dye (at 518 nm), the excited-state electrons of FITC dye may directly transfer to the lowest unoccupied molecular orbital (LUMO) of the 525-nm band of TNT−amine complex (part 2 of Figure 2B). Similarly, the excited-state electrons of ROX dye may transfer to the LUMO of the 630-nm band of TNT−amine complex (part 3 of Figure 2B). However, the resonance energy transfer is a predominant quenching process in the case of the TNT−amine complex and greatly amplifies the fluorescence-quenching response to TNT analyte (refer to the text hereinafter).

Dye-(NH_2)-Silica Nanoparticles. The silica nanoparticles with a hybrid monolayer of dye molecules and amine ligands were prepared by the procedure described in the Experimental Section. The SEM image of Figure 3A shows that the silica nanoparticles are still highly spherical and monodisperse, and the surface of particles is very smooth after the chemical modification by the examination of TEM. The infrared spectra display the characteristic peak of amino groups at the range of 1440−1460 cm^{-1} (data not shown), indicating the presence of amine ligands at the surface of silica nanoparticles. The solutions of FITC-(NH_2)-silica and ROX-(NH_2)-silica particles display the visible absorption peaks of dye fluorophores with the λ_{max} at 502 and 560 nm, respectively, as indicated with arrows in Figure 3B. The colorful dotted lines of Figure 3B shows the emission spectra of (1) FITC-(NH_2)-silica and (2) ROX-(NH_2)-silica particle solutions. FITC-(NH_2)-silica particles display a green fluorescence emission with λ_{max} at 518 nm (excited at 470 nm), and ROX-(NH_2)-silica nanoparticles display a red emission with λ_{max} at 602 nm (excited at 530 nm), which are identical to the emission spectra of corresponding pure dyes. Meanwhile, we can see that the solutions of FITC-(NH_2)-silica and ROX-(NH_2)-silica nanoparticles display bright green and red fluorescence under a UV lamp, respectively (inset images of Figure 3B). These observations clearly indicate that the hybrid monolayer of dye molecules and amine ligands is very stable and highly productive, ensuring that the nanoparticles have a strong surface affinity to TNT and a high fluorescence brightness for the ultratrace detection of TNT.

Fluorescence Responses of Dye-(NH_2)-Silica and Dye-Silica and Pure Dye to TNT. Part A of Figure 4 shows the fluorescence responses of FITC-(NH_2)-silica and FITC-silica particles and pure FITC dye to TNT analyte in solution. The fluorescence intensities decrease with increasing successive aliquots of TNT concentrations in the three forms of FITC dye systems. However, it was clearly detected that the fluorescence quenching of FITC-(NH_2)-silica particles is much larger than that of the FITC−silica particles without the free amine ligands at surfaces. Moreover, pure FITC dye only exhibits a very slight fluorescence quenching with TNT analyte, and the quenching efficiency of FITC dye is the lowest in the three forms of FITC dye systems. The order of quenching efficiency with TNT is FITC-(NH_2)-silica ≫ FITC−silica > pure FITC. Meanwhile, part B of Figure 4 shows that a similar order of quenching efficiency is also observed for the three corresponding forms of ROX dye systems: ROX-(NH_2)-silica ≫ ROX-silica > pure ROX. These measurements confirm that the primary amine ligands can greatly enhance the quenching efficiency of fluorescence, amplifying the spectral sensitivity of the dye molecule to the TNT analyte. In the case of dye-(NH_2)-silica nanoparticles, the electron-rich amine ligands can adsorb the electron-deficient nitroaromatics onto the surface of the silica nanoparticles through formation of TNT−amine complexes, as described in Figure 2A. Therefore, the dye-(NH_2)-silica nanoparticles have a higher affinity to TNT than dye−silica nanoparticles, leading to a higher quenching percentage. In the case of dye−silica nanoparticles without the free amine ligands, the large surface area of nanoparticles can also provide a weak enriching effect to TNT species. The quenching percentage of dye−silica nanoparticles is thus higher than that of pure dye. By comparing part A with B, however, we can clearly find that the quenching efficiency of FITC-(NH_2)-silica particles is obviously higher than that of ROX-(NH_2)-silica particles, although the quenching efficiencies of pure FITC and ROX dyes are almost equal under the same condition. These strongly suggest that the mechanism of fluorescence quenching of dye-(NH_2)-silica nanoparticles is quite different from that of corresponding pure dyes in solution.

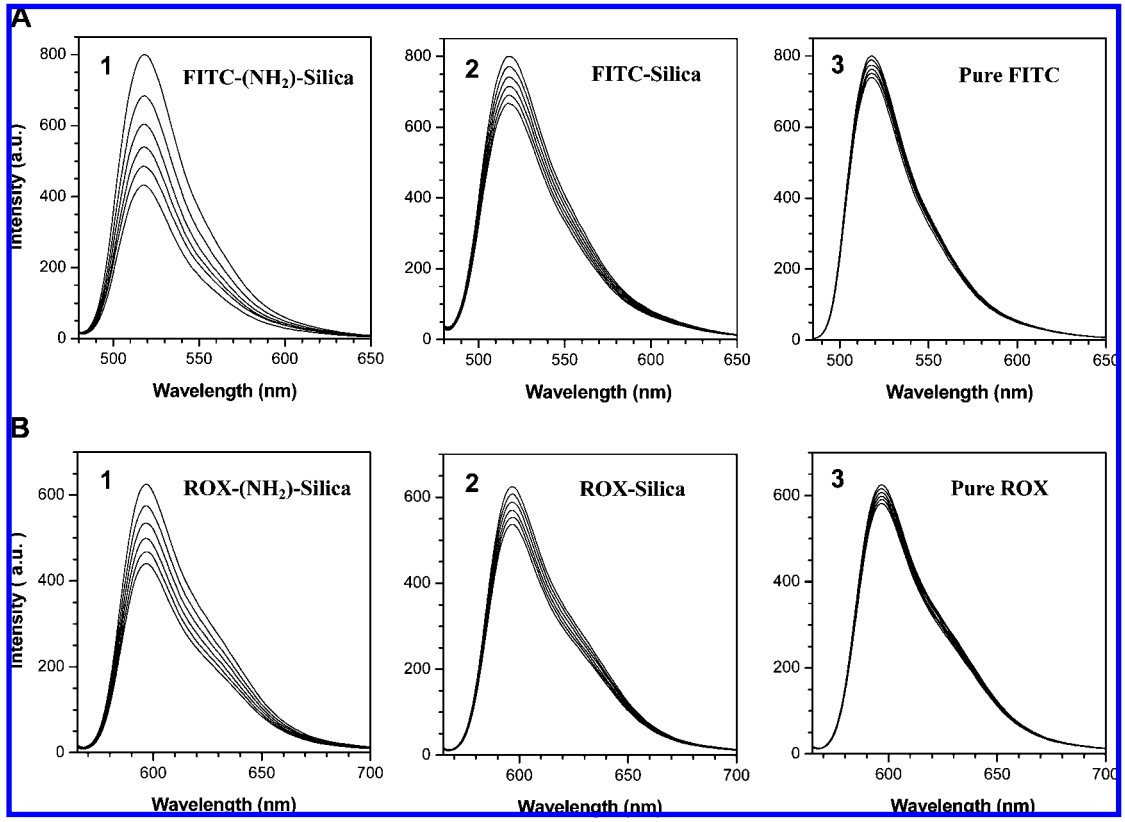

Figure 4. Evolution of fluorescence spectra of (A) FITC-(NH_2)-silica (1), FITC-silica (2), and pure FITC (3), and (B) ROX-(NH_2)-silica (1), ROX-silica (2),and pure ROX (3) with increasing TNT concentration. The concentrations of TNT from top to bottom are 0, 20, 40, 60, 80,and 100 μM, respectively. The amount of silica particles is 20 μg/mL in solution.

Table 1. Summary of Quenching Constants K_{sv} with TNT, DNT, NB, and RDX Analytes in Solution

		K_{sv}			
	λ_{exc} (nm)	TNT	DNT	NB	RDX
FITC-(NH_2)-silica	470	9038	2072	2035	2011
FITC−silica	470	1991	1951	1875	1730
FITC	470	813	707	692	659
ROX-(NH_2)-silica	530	4195	1761	1730	1659
ROX−silica	530	1666	1650	1638	1608
ROX	530	727	713	677	668

Confirmation of FRET-Amplifying Quenching Mechanism. To explore the fluorescence quenching mechanism of dye-(NH_2)-silica nanoparticles with TNT, the Stern−Volmer equation was used to evaluate the differences in quenching efficiency for these three forms of FITC and ROX systems, respectively, as follows: $(I_0/I) - 1 = K_{SV}$ [TNT], where I_0 is the initial fluorescence intensity in the absence of analyte, I is the fluorescence intensity in the presence of [TNT], and K_{SV} is quenching constant with TNT. Figure 5 shows the Stern−Volmer plots of (A) FITC-(NH_2)-silica and ROX-(NH_2)-silica, (B) FITC−silica and ROX−silica, and (C) FITC and ROX, respectively. A linear Stern−Volmer relationship is observed at the TNT concentrations lower than 1×10^{-4} M for these dye systems. The comparison of K_{SV} values was given in Figure 5D. The quenching constants of FITC-(NH_2)-silica and ROX-(NH_2)-silica particles are 9038 and 4195 M^{-1}, respectively. Therefore, the quenching efficiency of FITC-(NH_2)-silica is 2.15-fold that of ROX-(NH_2)-silica particles. It is particularly interesting that this ratio of quenching constants is almost equal to the ratio of mole extinction coefficients of the TNT−amine complex at the maximum emission wavelengths of FITC and ROX (at 518 and 602 nm). As shown in the absorption spectrum of the TNT−amine complex (Figure 1B), the ratio of extinction coefficient at 518 nm to that at 602 nm is ~2.0. However, Figure 5D shows that the K_{SV} values of pure FITC and ROX dyes with TNT is very small and almost equal at the same condition. Moreover, the quenching constant of FITC−silica particles is only slightly larger than that of ROX−silica particles. These results strongly suggest that the fluorescence emission of dye-(NH_2)-silica nanoparticles is absorbed by the formed TNT−amine derivatives at the silica surface, leading to the FRET behavior from dye donor to nonemissive TNT−amine acceptor through their polar−polar interactions at near proximity, as illustrated in Figure 2B.

The linear relationships of Stern−Volmer plots suggest that the quenching arises from either a static mechanism by the quenching of a bound complex or a dynamic mechanism by the quenching of a bimolecular collision of the excited states. In the case of dye-(NH_2)-silica particles, the interactions between TNT and amine ligands lead to the strong adsorption of TNT at the surface of silica particles. The inset of Figure 5A also shows that the fluorescence lifetime of FITC-(NH_2)-silica keeps almost invariant as the concentration of TNT is increased, confirming that static quenching is a predominant process.[5] Therefore, a most possible explanation on these above observations is that the fluorescent emission of dye molecules is quenched by the TNT−amine complexes bound at the surface of nanoparticles.

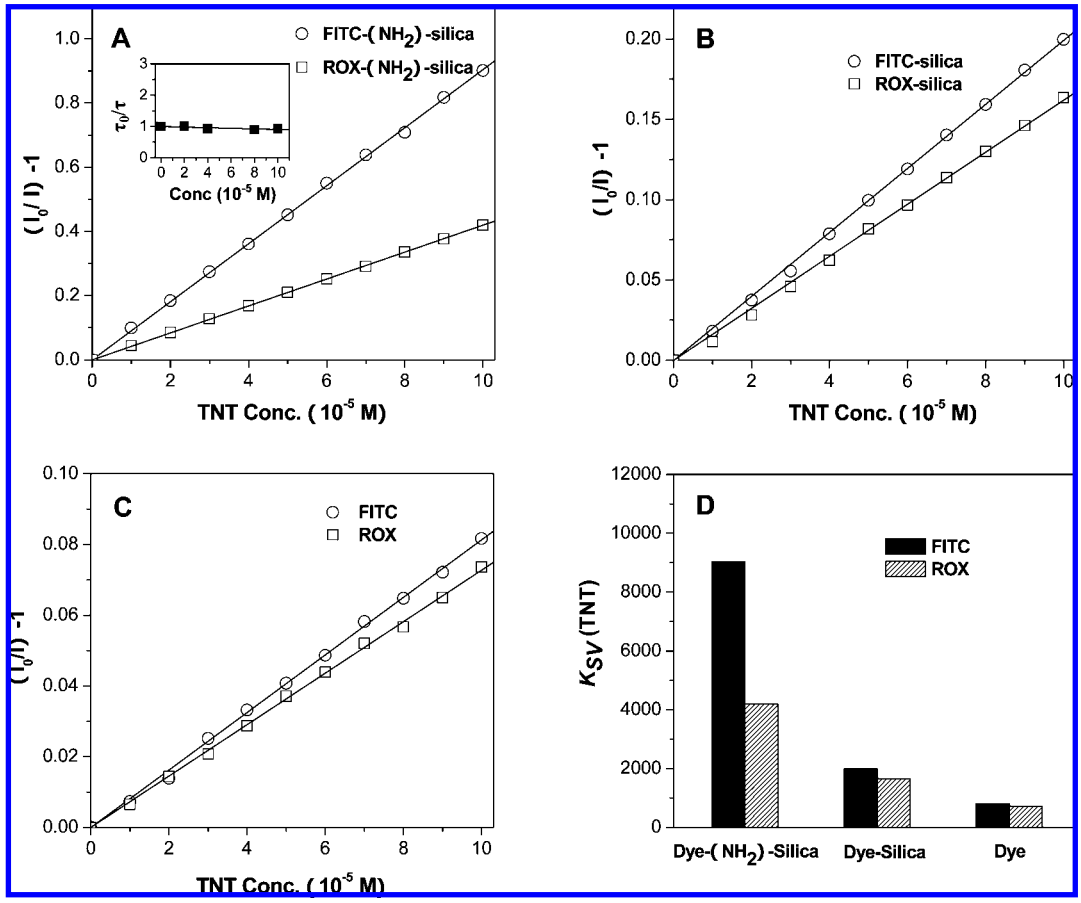

Figure 5. Stern−Volmer plots from (A) dye-(NH_2)-silica nanoparticles, (B) dye−silica nanoparticles, and (C) pure dyes with TNT in solution. (D) Quenching constants (K_{sv}) of dye-(NH_2)-silica, dye−silica, and pure dyes. The inset in (A) is the plot of fluorescence lifetime (τ/τ_0) vs TNT concentrations for FITC-(NH_2)-silica nanoparticles.

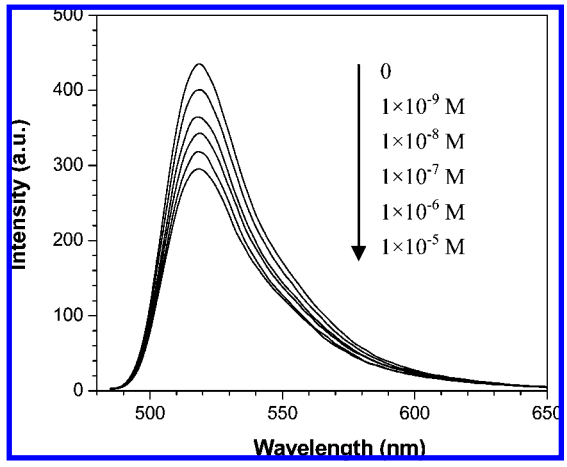

Figure 6. Evolution of fluorescent intensity with increasing ultratrace amounts of TNT into 2 mL of the suspension containing 20 μg of FITC-(NH_2)-silica nanoparticles.

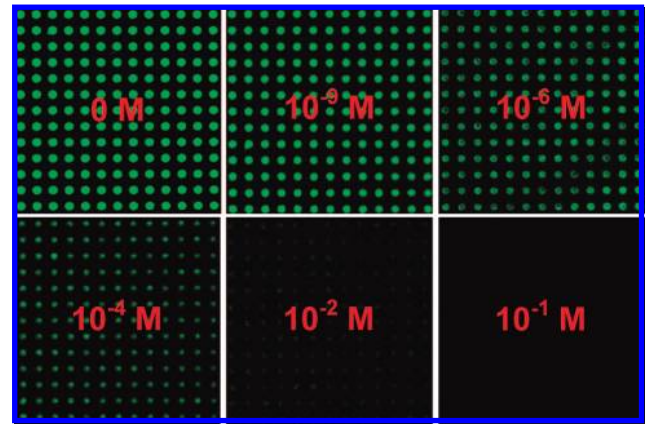

Figure 7. Regular array assembly of FITC-(NH_2)-silica nanoparticles on the silicon wafer with etched microwells. Confocal fluorescence images show the evolution of the brightness and size of fluorescent dots on dropping 10 μL of TNT solution of different concentrations.

Figure 5D shows that the K_{SV} values of pure FITC and FITC−silica particles are only 813 and 1991 M^{-1}. The quenching constant of FITC-(NH_2)-silica particles (9038 M^{-1}) is ~11- and ~4.5-fold those of FITC dye and FITC−silica particles, respectively. Meanwhile, the quenching constant of ROX-(NH_2)-silica particles is ~5.8- and ~2.5-fold that of ROX and ROX−silica particles, respectively. That is to say, the hybrid monolayer of dye molecules and amine ligands at the surface of silica nanoparticles greatly amplified the quenching response of dye to TNT for both the FITC and ROX systems. However, the amplified efficiency for FITC systems is much larger than that for the ROX system, which is consistent with our expectation. Therefore, the comparisons further confirm that the large fluorescence quenching of FITC-(NH_2)-silica particles with TNT mainly results from the highly efficient FRET from the FITC fluorophores to the TNT−amine complexes, due to the whole spectral overlapping

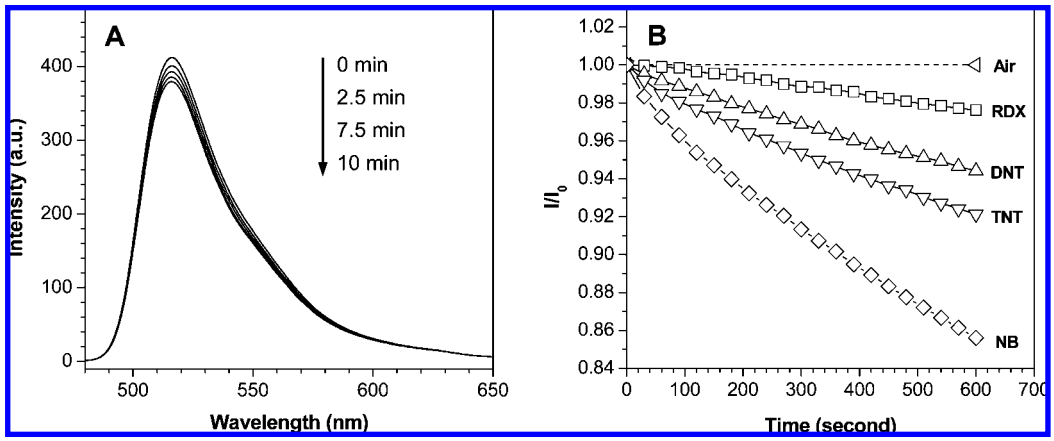

Figure 8. (A) Evolution of fluorescent intensity of FITC-(NH_2)-silica particle film on exposure to TNT-saturated air (~4 ppb) for the indicated time periods. (B) The variation of the quenching percentage for FITC-(NH_2)-silica particle film as a function of the time of exposure to the saturated vapor of different nitro analytes.

as shown in Figure 1B. The spatial proximity between TNT-binding sites and FITC fluorophores can ensure the communication between these two kinds of active components without the need for any direct covalent linkage between them.

Quenching Efficiency with Other Nitrocompounds. We further tested the quenching response of the two kinds of dye systems to DNT, NB, and RDX, which are structural analogues of TNT. As listed in Table 1, the quenching constants of FITC-(NH_2)-silica and ROX-(NH_2)-silica particles with TNT are much larger than those with DNT, NB, and RDX, respectively. Moreover, the fluorescent silica particles with and without amine ligands does not exhibit any obvious difference in quenching constants with DNT, NB, and ROX, respectively. The quenching constants of pure FITC and ROX dyes for an identical nitro compound are also almost equal. These are again consistent with our expectation that the highest fluorescence quenching of FITC-(NH_2)-silica particles with TNT is closely related to the formation of TNT−amine complexes at the surface of silica. It is well-known that DNT and NB are much weaker Lewis acids or electronic acceptors than TNT molecules.[7] Although the weak interactions may lie between amine ligands and DNT or NB molecules, the UV−visible spectra do not detect any visible absorption peak when DNT or NB is added into the solution of APTS. This suggests that DNT and NB molecules cannot likely form the effective Meisenheimer complex with amine ligands.[9] Meanwhile, RDX does not have any specific interaction with amine ligands. On the other hand, Table 1 also shows that the quenching constants of FITC−silica and ROX–silica particles with DNT, NB, and RDX are greater than the corresponding pure dyes, respectively. This is mainly because the large surface-to-volume ratio of silica nanoparticles can play a role in the enrichment of analytes from solutions. All above results further confirm that the FITC-(NH_2)-silica nanoparticles exhibit the highest fluorescence sensitivity and chemical selectivity for TNT analyte, due to the formation of the TNT−amine complex at the silica surface and the highly efficient FRET-based quenching.

Detection of Ultratrace TNT in Solution. The FRET-amplifying quenching of FITC-(NH_2)-silica nanoparticles is applicable to detect ultratrace TNT analyte. The detection was carried out with a lower concentration of FITC-(NH_2)-silica nanoparticles such as 10 μg/mL, because the silica particles have a very high brightness of fluorescence to meet the requirements of fluorescent measurements. Figure 6 shows the evolution of fluorescent intensities with increasing ultratrace amounts of TNT in the solution of FITC-(NH_2)-silica nanoparticles. The fluorescence of nanoparticles was gradually quenched with the addition of TNT. We can see that 1 nM TNT in solution was detected as an ~8% decrease in the fluorescence intensity, which is larger than the reported detectable standard of 5% decrease in intensity.[14] Accordingly, the attenuation of fluorescence intensity can clearly be detected down to 1 nM TNT in solution at least.

Nanoparticle-Assembled Chips for Ultrasensitive Detection of TNT. Meanwhile, we develop the inexpensive solid-state chips for ultrasensitive detection of TNT explosive by assembling the FITC-(NH_2)-silica nanoparticles into the etched microwell array of the silicon wafer. When the aqueous suspension of FITC-(NH_2)-silica nanoparticles was cast onto the silicon chip with etched microwells of 5 μm in diameter and 2 μm in depth and dried under ambient condition, the microwells were spontaneously filled with the silica particles. Figure 7 shows the colorful fluorescence images under laser excitation on a confocal microscope. The fluorescent dot array is highly regular and extremely bright, and all microwells are completely filled with the fluorescent silica particles. The evolution of the brightness and size of fluorescent dots is clearly observed by dropping only 10 μL of TNT solution of different concentrations onto the 1 × 1 cm^2 sized chip. The brightness and size of fluorescent dots become smaller and smaller and ultimately disappear with the increase of concentration from 1×10^{-9} to 10^{-1} M. However, the nanoparticle chip seems to have a more sensitive response to the ultratrace amount of TNT than the nanoparticle suspensions. As shown in the Figure 7, 10 μL of 1 nM TNT can result in a surprising reduction of the brightness and size of fluorescent dots under confocal microscope. It is thus estimated that ~2 pg of TNT can clearly be detected using the nanoparticle-assembled chip. Moreover, one of the main advantages of the detection chips is that less amount of sample is needed for an ultratrace-level detection, due to the collective effect of particle assembly in the microwells. Therefore, the microchips can be used as a convenient indicator of TNT residues.

Detection of TNT Vapor. Meanwhile, there has been considerable interest in the detection of nitro aromatic vapors.

The FITC-(NH_2)-silica nanoparticles can also strongly adsorb TNT vapor from atmospheric phase by the specific interactions of TNT with amine ligands and exhibit an amplifying quenching response. We thus used FITC-(NH_2)-silica nanoparticles to fabricate the thin-film-based fluorescence sensor for the detection of TNT vapor. The silica particle suspension was simply coated onto a piece of filter film and dried at ambient temperature. A control experiment using the film sensor with air produced no significant decrease in photoluminescence intensity. The dynamic quenching was measured under the saturated vapor of TNT in air. Figure 8A shows the fluorescence spectra of the nanoparticle film exposed to 4 ppb TNT vapor in air. The fluorescence intensity decreases with increasing the time of exposure to TNT vapor. Figure 8B shows the variation of the quenching percentage as a function of the time of exposure to the TNT, DNT, NB, and RDX vapors. After ~10 min, the quenching percentage of fluorescence was ~8% for TNT-saturated air (vapor pressure, 4 ppb at 25 °C), only 5% for DNT-saturated air (vapor pressure, 200 ppb at 25 °C), 15% for NB-saturated air (vapor pressure, 400 ppm at 25 °C), and 2% for RDX-saturated air (vapor pressure, 0.0084 ppb at 300 K). Because the vapor pressures of DNT and NB are about 50- and 1×10^5-fold that of TNT, respectively, the quenching percentage with TNT vapor is thus surprisingly larger than that expected from the relative vapor pressure of these analytes. The enhanced sensitivity toward TNT vapor originates from the extremely strong adsorption of TNT species at the amine ligands and the efficient FRET-based quenching. Moreover, the large surface-to-volume ratio of nanoparticles is also an advantageous factor to enhance the specific interaction between TNT species and the amine ligands, maximizing the quenching efficiency of fluorescence.

CONCLUSIONS

We have demonstrated the resonance energy transfer-amplifying fluorescence quenching toward the ultrasensitive detection of TNT by the use of a hybrid monolayer of dye fluorophores and amine ligands at the surface of silica nanoparticles. The primary amine ligands at the surface of silica particles can specifically bind TNT species from the environment by the formation of a TNT−amine complex. Meanwhile, the nonemissive FRET between the dye and the resultant TNT−amine complex in spatial proximity leads to an enhanced quenching response. The two basic processes have achieved the ultrasensitive detection of TNT in solution and atmosphere and selectively distinguished TNT from other types of nitro compounds. The nonemissive FRET-based nanoparticle sensors have several remarkable advantages as follows: (1) facile preparation without use of complicated chemical procedure; (2) extremely high fluorescence brightness suited well for the detection of ultratrace analytes; (3) high specificity and sensitivity to target species; (4) easy assembly into a large-area regular array in practical applications. In addition, the simple FRET-based strategy may be extended to the design of chemosensors of other analytes such as metal ions and biological molecules.

ACKNOWLEDGMENT

We thank Mr. Xiaoyong Deng (Shanghai University) and Dr. Hongbing Fu (Institute of Chemistry, CAS) for their help in experiments of confocal microscope and fluorescence lifetime spectroscopy, respectively. This work was supported by Natural Science Foundation of China (20875090, 60771036) and 863 high technology project of China (2007AA10Z434) and National Basic Research Program of China (2006CB300407), and Innovation Project of Chinese Academy of Sciences (KJCX2-SW-W31). We also thank the Hundreds Talent Program of the Chinese Academy of Sciences for financial support.

Received for review July 11, 2008. Accepted September 8, 2008.

AC8014356